

UC Merced

UC Merced Previously Published Works

Title

Evapotranspiration Mapping for Forest Management in California's Sierra Nevada

Permalink

<https://escholarship.org/uc/item/4kb947md>

Authors

Roche, James W
Ma, Qin
Rungee, Joseph
et al.

Publication Date

2020-05-13

DOI

10.3389/ffgc.2020.00069

Peer reviewed

Evapotranspiration mapping for forest management in California's Sierra Nevada

James W. Roche^a, Qin Ma^{b,c}, Joseph Rungee^c, Roger C. Bales^{c*}

^aNational Park Service, Torrey, UT. ^bDepartment of Forestry, Mississippi State University, MS. ^cSierra Nevada Research Institute, University of California, Merced. *Corresponding author.

ABSTRACT

We assessed the response of densely forested watersheds with little apparent annual water limitation to forest disturbance and climate variability, by studying how past wildfires changed forest evapotranspiration, and what past evapotranspiration patterns imply for the availability of subsurface water storage for drought resistance. We determined annual spatial patterns of evapotranspiration using a top-down statistical model, correlating measured annual evapotranspiration from eddy-covariance towers across California with NDVI (Normalized Difference Vegetation Index) measured by satellite, and with annual precipitation. The study area was the Yuba and American River watersheds, two densely forested watersheds in the northern Sierra Nevada. Wildfires in the 1985-2015 period resulted in significant post-fire reductions in evapotranspiration for at least 5 years, and in some cases for more than 20 years. The levels of biomass removed in medium-intensity fires (25-75% basal area loss), similar to magnitudes expected from forest treatments for fuels reduction and forest health, reduced evapotranspiration by as much 150-200 mm yr⁻¹ for the first 5 years. Rates of recovery in post-wildfire evapotranspiration confirm the need for follow-up forest treatments at intervals of 5-20 years to sustain lower evapotranspiration, depending on local landscape attributes and interannual climate. Using the metric of cumulative precipitation minus evapotranspiration (P-ET) during multi-year dry periods, we found that forests in the study area showed little evidence of moisture stress during the 1985-2018 period of our analysis, owing to relatively small reliance on interannual subsurface water storage to meet dry-year evapotranspiration needs of vegetation. However, more-severe or sustained drought periods will push some lower-elevation forests in the area studied toward the cumulative P-ET thresholds previously associated with widespread forest mortality in the southern Sierra Nevada.

INTRODUCTION

Understanding and predicting how forests respond to disturbance is important for managing source-water areas, particularly in semi-arid climates, which have a high ratio of evapotranspiration to precipitation. This is an immediate concern where a combination of a warming climate and past management has contributed to: i) high wildfire extent and intensity (McKenzie et al., 2004; North et al., 2015a; Westerling, 2006), ii) drought-related forest mortality (Allen et al., 2010; Anderegg et al., 2013, 2015; Bales et al., 2018), and iii) reduced runoff (Barnett et al., 2005; Goulden & Bales, 2014). The response of evapotranspiration to disturbance and interannual changes in temperature and precipitation is relatively muted compared to runoff, making it a potentially convenient metric for changes in water balance from forest management. Thus it is urgent to improve our understanding and accurate mapping of evapotranspiration response to changes in forest vegetation, which dominates that response (Bosch & Hewlett, 1982; Naudts et al., 2016; Saksa et al., 2017).

As forests are dynamic systems, water use by forests can respond in multiple ways to reductions in biomass (Tague et al., 2018). For example, Saksa et al. (2019) reported a significant reduction in evapotranspiration following fuels treatment in a densely forested central Sierra Nevada area, but no significant reduction in a comparable but more water-

limited southern Sierra area. In the southern site, reductions in forest biomass apparently stimulated growth of remaining vegetation. Forest regrowth following disturbance is also quite variable (Roche et al., 2018; Tague and Moritz, 2019; Tague et al., 2013).

While multiple interacting and non-linear factors affect evapotranspiration, as reflected in physics-based models (Chen et al., 2005; Running et al., 1987) and bottom-up modeling blended with remote-sensing data (Mu et al., 2011; Baldocchi et al., 2019), it is also possible to consider their net effects in top-down approaches, particularly over multi-year timescales (Sivapalan et al., 2003). With the advent of high-confidence spatial-evapotranspiration estimates driven by a robust empirical relation between satellite-derived estimates of vegetation greenness, represented by normalized difference vegetation index (NDVI), and point measurements of evapotranspiration in a variety of ecosystems (Goulden et al., 2012; Goulden and Bales, 2019), it is possible to estimate the water balance with high spatial resolution across forested mountain landscapes. In the context of forest management, this tool permits estimation of evapotranspiration change resulting from past fuels treatments and wildfire (Roche et al., 2018), and projecting changes from future treatments and disturbance. This data-driven, top-down statistical approach complements more-detailed bottom-up hydrologic modeling, which generally uses

precipitation and streamflow as the main state variables to infer changes in evapotranspiration as forest vegetation changes (Zierl et al., 2007). The empirical-statistical approach is also attractive for basin-scale or smaller studies, where remote-sensing-based evapotranspiration products that were largely designed for global and large regional applications perform poorly (Goulden et al., 2012).

Further, extending the work of Fellows and Goulden (2017), it is possible to map the spatial variability in the amount of subsurface water storage required to sustain evapotranspiration during both dry seasons and during multi-year droughts, thereby identifying areas with greater or lesser drought resistance and/or potential benefit from thinning treatments (Rungee et al., 2019; Klos et al., 2018).

Forest management for fuels treatments in the Sierra Nevada and other overstocked forests is widely regarded as a necessary step to reduce the probability of high-intensity wildfire, restore forest health, and return forests to a more-sustainable condition following a century of fire suppression (Miller et al., 2012; North et al., 2015a). While fuels and forest-health concerns may be the primary drivers for fuels treatments, other benefits can be important contributors to the collaborations needed to implement forest-restoration projects. Valuing and monetizing water-related benefits requires credible, accessible metrics for both planning and verification.

The aim of the research reported here is to assess the response of a densely forested mountain watersheds with little apparent annual water limitation to forest disturbance and climate variability. Two questions motivated this work. First, what changes in evapotranspiration and water balance across these densely forested areas have occurred from historical disturbances by wildfire, and post-fire regrowth. Second, what magnitude of subsurface water storage have these forests historically used to continue growth during seasonally and multiyear dry periods; and what future vulnerabilities do the spatial patterns of these water balances reveal.

METHODS

In the analysis of water-balance changes from wildfire, we focused on evapotranspiration (ET) patterns in the Yuba and American River watersheds (Figure 1), two densely forested basins with significant annual runoff and multiple downstream services that depend on that runoff, yet high potential for severe wildfire and disruption of those services. Vegetation in the study area goes from grassland and

oak savannah at lower elevations, through pine-oak forest, mixed-conifer forest, and subalpine at higher elevations. The 4825 km² American basin experienced 5 wildfires over 4000 ha (9884 ac) in area during our 1985-2018 study period, with the largest being the 2014 King Fire (37,315 ha) (Tables S1-S2). Much of the area burned in these large fires was in dense, productive mixed-conifer forests, with overall wildfire elevations spanning 600-2200 m. Only one fire over 4000 ha occurred in the 2870 km² Yuba, the 1999 Pendola Fire (4408 ha, 467-1028 m elevation). There were several smaller fires in both watersheds. Using California Wildlife Habitat Relationship System data (<https://wildlife.ca.gov/Data/CWHR>), 77% of burned area may be classed as mixed conifer (Sierra Mixed Conifer, White Fir, Jeffrey Pine, Ponderosa Pine, Montane-Hardwood-Conifer, Montane Chaparral), 15% is Montane Hardwood, and 3% is Perennial Grasslands (Figure 1).

We determined annual spatial patterns of evapotranspiration using a top-down statistical model (Goulden and Bales, 2014; 2019), and used published gridded data for precipitation (P). Using a pixel-by-pixel annual water balance ($P = ET + Q - \Delta S$), we evaluated spatial values of $P - ET$ to estimate gridded runoff (Q) and change in annual subsurface storage (ΔS) following Bales et al. (2018). We evaluated the basin-scale water balance by summing $P - ET$ across each basin and comparing with published values of whole-basin runoff.

We examined the impact that wildfire has had on evapotranspiration using the methods of Roche et al. (2018), and estimated the spatial patterns of subsurface water demand using the methods of Fellows and Goulden (2017). Finally, we show how this approach can be used to project potential evapotranspiration reductions for the level of fuels treatments proposed to restore forests to a more-sustainable state.

Gridded evapotranspiration. To prepare components of the water balance for the Yuba-American region, we first assembled water-year (October – September) annual means of NDVI from Landsat data for 1985-2018. Annual means incorporated USGS Landsat Collection 1 Tier 1 surface-reflectance data (30-m resolution) from Landsat 5 (1985-2011), Landsat 7 (2012-2013), and Landsat 8 (2014-2018) missions, filtered for clouds, cloud shadows, water, and snow. Additional filtering for shadows was accomplished by masking pixels for which values in the red, shortwave infrared 1, and shortwave infrared 2 bands were less

than 1%, and values in the infrared band were less than 5% reflectance. All NDVI grids derived from Landsat 7 (L7_{ETM+}) and Landsat 8 (L8_{OLI}) were then homogenized to Landsat 5 Thematic Mapper (L5_{TM}) using the methods of Su et al. (2017), by the following equations:

$$L5_{TM} \times 100 = 0.9883 \times L7_{ETM+} \times 100 - 3.665 \quad (1)$$

$$L5_{TM} \times 100 = 0.82128 \times L8_{OLI} \times 100 + 0.027719 \quad (2)$$

Assembling the NDVI means and homogenization was completed in the Google Earth Engine cloud-computing environment (Google Earth Engine Team, 2015), and products were exported for further processing as described below.

Annual mean NDVI raster datasets were converted to estimates of annual evapotranspiration building on the methods of Goulden and colleagues, who provide rationale for using a statistical versus energy-balance approach to extrapolate ET in complex terrain like that found in the Sierra Nevada (Goulden et al., 2012). They note that previous investigators have shown that in semi-arid regions, a site's water balance, Leaf Area Index (LAI), primary production, and annual ET are tightly correlated through a series of feedbacks, with a high LAI both driving a high annual ET and symptomatic of a location with a high ET (Grier and Running, 1977; Gholz, 1982). They also note that LAI has been shown to be well correlated with NDVI (Carlson and Ripley, 1997), creating a tight relationship between NDVI and ET, with previous studies confirming a strong correlation between annual ET and NDVI across semi-arid landscapes (Groeneveld et al., 2007). Goulden et al. (2012) further note that alternatively, physically based approaches to scaling ET require spatially resolved radiation, temperature, humidity, wind speed, and other attributes that vary markedly over small distances, making extrapolation of montane meteorological conditions to fine scale highly uncertain. We thus use their simpler approach of regressing ET against a vegetation index.

Because our focus is on wetter regions than most of the calibration data used previous studies, we extended the calibration to include three sites with higher precipitation that are in or near the study area (see Supplement for details). Specifically, we evaluated two calibrations: i) an extension of the two-parameter exponential regression used previously (Roche et al., 2018; Bales et al., 2018) that has been applied previously for disturbance analysis, and ii) a multiple regression using NDVI and precipitation

aimed at better representing basin-wide water balance. Using leave-one-out cross validation to assess the model temporal sensitivity, we found that most predictions fall within ± 100 mm yr⁻¹ of measurements, with the main exceptions being points at high NDVI where saturation is an issue (see Figures S1-S2 for data and calibrations).

Eddy covariance is a well-accepted measurement method, yet it remains important to consider uncertainties. Analysis of cumulative ET and carbon dioxide (CO₂) fluxes shows that there is no single definition or single cause of uncertainty (Goulden et al., 1996). The uncertainty in ET fluxes, estimated to be up to 10%, is driven by uncertainty in the assumption that the Bowen Ratio is correct, uncertainty in soil and other heat-storage terms, and to a lesser extent net radiation. Sampling uncertainty should be about 5%, similar to that estimated for CO₂. Thus the uncertainty of annual ET from an individual tower is as much as 15%. This uncertainty should be random from tower to tower, and to a lesser extent year to year, so the overall uncertainty should be less for the full dataset. Calibration with NDVI may introduce another 5%, leading to an overall uncertainty in the model of at least 10% but less than 20%.

Fire effects on evapotranspiration. Using the estimate of annual *ET* derived above, we estimated the elevational and cumulative *ET* effects of large fires, >50 ha, as assembled by Region 5 of the U.S. Forest Service (1990-2017; https://www.fs.usda.gov/Internet/FSE_DOCUMENTS/fseprd596284.zip) in these watersheds using the methods of Roche et al. (2018). Fire statistics are shown in Tables S1-S2. We chose to examine the impacts of fires for 1990-2013 in order to incorporate a five-years-before-fire estimate of *ET* from the Landsat record, which begins in 1985, and similarly estimate the five-years-post-fire mean *ET* (up to the year 2018). Given that overlapping fire perimeters accounted for less than 2% of the area burned, we combined all fire polygons into a single layer, attributing overlap areas with information pertaining to the earliest fire to occur in the 1985-2017 period. This layer was overlain with a 100-m grid that was buffered from the fire perimeters by 75 m to minimize the influence of partially burned grid cells. Each grid cell was additionally attributed with the year of the fire, mean elevation, mean percent change in basal area one-year post fire using Miller et al. (2009) and Miller and Quayle (2015),

(https://www.fs.usda.gov/Internet/FSE_DOCUMENT/S/fseprd596279.zip) and mean estimated *ET* for each water year. We created a similar database of unburned 100 × 100 m polygons that comprised 20% of forested area in each watershed over the period 1985–2018. A polygon was designated ‘forested’ if the majority of 30-m grid cells intersected by the polygon were classified as forest (deciduous, evergreen, or mixed-forest classes) in the 2011 USGS National Land Cover Database (Homer et al., 2015). The actual change in *ET* for each grid cell was estimated for each year post fire until post-fire *ET* equaled or exceeded pre-fire *ET*, or until 2018:

$$\text{Annual } ET \text{ reduction} = ET_{\text{burned, 5-years-pre-fire-mean}} - ET_{\text{burned, post-fire}} - (ET_{\text{unburned, 5-years-pre-fire-mean}} - ET_{\text{unburned, post-fire}}) \quad (3)$$

Estimates of the unburned control *ET* were a mean of all unburned polygons in a 500-m elevation band centered on each burned grid cell in each major watershed.

Using this dataset, we then estimated changes in evapotranspiration by forest basal-area reduction (burn severity) class (0–25%, 25–50%, 50–75%, and 75–100%) and elevation (by 100-m elevation band) by comparing the 5-year post-fire mean *ET* with the 5-year pre-fire mean *ET*. We also estimated net annual evapotranspiration change across all burned areas for the period 1990–2018 as well as recovery rates by burn-severity class as reported by the USFS.

Subsurface water balance. In order to estimate the amount of soil water extracted from storage each year, we used the methods of Fellows and Goulden (2017), which follows methods outlined by Lutz et al. (2010). The steps are: i) estimate monthly water input to the soil water index using monthly 800-m PRISM (Parameter-elevation Relationships on Independent Slopes Model, PRISM Climate Group, 2019) precipitation data and an estimate of snowmelt (see Lutz et al., 2010), ii) calculate monthly potential evaporation (PET) using monthly mean temperature from PRISM and the modified Hamon (1963) method employed by Lutz et al. (2010), and 3) combining estimates of actual evapotranspiration from NDVI regression with water indices and PET, by subtracting the annual sum of monthly minimums of water indices and PET from *ET* values. All calculations were done at 30-m resolution. We used the time series of PRISM precipitation data at a resolution of 800 m for the study period. We downsampled these layers to 30 m by nearest-neighbor interpolation, summed by water

year, and aligned the resulting grids with the above *ET* raster. We averaged daily minimum and maximum temperature using 800-m PRISM data, then created monthly means, and finally downsampled the monthly temperature layers to 30 m by nearest-neighbor interpolation. Estimates of PET using the method of Hamon as outlined in Dingman (2002) were modified as follows:

$$PET = 1.265 \times PET_{\text{Hamon}} \quad (4)$$

where 1.265 is a tuning factor used by Fellows and Goulden (2017) to minimize bias between PET and *ET* datasets. Snowpack was set to zero each year, i.e. no year-to-year carryover of snowpack storage. Finally, we determined the maximum withdrawal from storage for each grid cell over the 1985–2018 period, which may be considered the minimum amount of subsurface water-storage capacity.

Basin-scale annual and interannual water balance.

We derived annual rasters of *P-ET*, an estimate of the amount of water available for runoff or storage recharge (excess) or the amount of water required from storage (deficit) to maintain estimated annual *ET*. Starting with the 1985 *P-ET* grid, we then tracked interannual use of water in storage by summing *P-ET* in each cell year by year. Negative values of *P-ET*, which indicate withdrawal from storage, were retained in any given year and positive values, indicating no withdrawal, were set to zero. In order to estimate a maximum amount of storage water used in any pixel during the 1985–2018 period, we extracted the lowest negative *P-ET* value from all storage-water-use grids.

We compared water-balance components using the above grids with full natural flow for the Yuba (Yuba River at Smartville, ID=YRS, California Data Exchange Center, 2019) and American (American River at Folsom, ID=AMF, California Data Exchange Center, 2019) River watersheds using the methods of Bales et al. (2018). For each watershed, we extracted annual *P*, *ET*, and depth of water extracted from soil storage (ΔS). The latter was determined as the mean of all grid cells where *P-ET* was negative. These components were compared to full natural flow (*Q*), using the annual water balance: $P = ET + Q - \Delta S$.

RESULTS

ET and precipitation by elevation band.

Evapotranspiration values peak in the Yuba and American at 700–800 mm yr⁻¹ around the 1100–1200 m elevation, whereas precipitation peaks at elevations closer to 1600–2000 m (Figure 2). Average precipitation (\pm stdev) is higher in the Yuba

(1479 ± 500), peaking near 1800 mm yr^{-1} at 2000 m elevation, compared to the American ($1228 \pm 430 \text{ mm yr}^{-1}$), peaking near 1500 mm yr^{-1} at 1700 m elevation. Volumetric runoff was calculated based on area per elevation band times runoff depth, and comes mainly from 800-2100 m elevation in the Yuba and 500-2100 m in the American (Figure 2). Evapotranspiration varied little between wet versus dry years, averaging about $675 \pm 57 \text{ mm}$ across the Yuba and $619 \pm 54 \text{ mm}$ in the American. The large interannual differences in precipitation, indicated by the coefficient of variation (CV) were amplified to give even larger relative interannual differences in $P-ET$. CV averaged 0.35 for precipitation and 0.63 for $P-ET$ across the 2 basins, whereas ET is similar in wet versus dry years ($CV=0.09$) (see also Figures S4-S5).

Effect of fire on ET . Reduced evapotranspiration due to all forest fires in the study area between 1990 and 2013 varied with respect to elevation and basal-area change (Figure 3). The mean annual ET during the five years post fire was reduced approximately $30\text{--}100 \text{ mm yr}^{-1}$ for each additional 25% reduction in basal area, between 750-2100 m elevation. This is most apparent in the American watershed, which had over 4 times the area burned as did the Yuba ($42,299$ vs 9850 ha) during this period (Tables S1-S2). Note that ET reduction varies within each burn-severity class, as illustrated for the 50-75% basal-area reduction class.

Post-fire recovery rates of ET were most rapid in the first 5 years, with approximate rates of $7\text{--}10 \text{ mm yr}^{-1}$, $7\text{--}13 \text{ mm yr}^{-1}$, and $9\text{--}13 \text{ mm yr}^{-1}$ for 0-25, 25-75, and 75-100% basal-area reduction, respectively (Figure 4). Evapotranspiration rates stabilized after 12 years in the Yuba and 15 years in the American. At 20 years post fire, there remained $50\text{--}90 \text{ mm yr}^{-1}$ ET reduction in the higher burn-severity classes in the American, while little post-fire effect was evident in the Yuba. Note that this analysis aggregated results over all fires analyzed; and variability in recovery rates within a severity class is quite large.

Differences in evapotranspiration reduction by fire and post-fire recovery between fires are illustrated for 4 large fires on Figure 5. The high severity of the Pendola fire did not translate to above-average ET reduction, which was $50\text{--}200 \text{ mm yr}^{-1}$, increasing with severity class. The area experienced a moderately long period to recover to pre-fire ET levels, with an average of 10.75 years. The percent area recovered was very high, averaging 78%. The area of the Star Fire had similar ET reduction, and has also experienced a high percentage of recovery, averaging 50%. This recovery

took an average of 13 years, which is also comparatively high. Of particular note is that these recovery metrics are relatively consistent across severity classes, i.e. ET in areas burned at low severity did not recover at a faster rate than did those experiencing higher-severity fire. We hypothesize that this is due to the forest in areas experiencing lower severity being less dense to start with. For the American Fire the ET reduction was similar, and there was a consistently shorter period to recovery, under five years across all severity classes. The area recovered is also very low, with a maximum of 12%, and decreases with increasing severity class. The much larger King Fire had a very significant five-year reduction in evapotranspiration, above 280 mm across all severity classes. It took two years to recovery for some areas in all severity classes, which is low. The area recovered is relatively high in the 25% severity class, and decreases with increasing severity.

Summing total ET reduction from one year post fire until recovery to pre-fire levels, we estimated the cumulative ET reduction for the period 1986-2018 for areas that burned 1985-2013, by fire by severity class. While the data are somewhat noisy, even after aggregating to 500-m elevation bands, given lack of uniform fire coverage by severity class within each basin, it is apparent that cumulative ET reduction generally exceeds 1200 mm for moderate fire severity (25-75% basal area reduction) in both basins and across a broad elevation range (500-2200 m) (Figure 6). Values are generally higher in the American across all severity classes except in the 750-m band in the highest severity class, which is the result of a single large fire.

Summed over the whole basin, the cumulative volumetric evapotranspiration reduction due to fires in the American watershed is more than 15 times that in the Yuba due to the extensive area burned in the American, particularly since 2013 (Figure 7a). Prior to 2013, ET reduction in the American peaked in 2009 at just over 40 million m^3 per year. This number more than tripled by 2015 due several large fires, including the American and Kings fires. The effect of the 2014 King Fire (largest polygon on Figure 1, running SSW to NNE in the center of the basin), is quite visible on the ET and $P-ET$ maps for 2015 (Figure S4). The Yuba watershed exhibited about $5\text{--}10$ million m^3 reduction per year. The net ET reduction for burned areas ranged between $50\text{--}240 \text{ mm yr}^{-1}$ depending on the size, basal-area reduction, and time since fire in each watershed (Figure 7b).

Maximum annual soil water use for

evapotranspiration. Much of the forested area in the watershed apparently has historically used 450–600 mm yr⁻¹ of subsurface water during the summer dry season each year to meet annual ET demand (Figure 8). Forests in the North Yuba accessed greater than 600 mm yr⁻¹, while forests at the highest elevations in both watersheds accessed less subsurface water due to a limited growing season. Lower values of subsurface water use at lower elevations reflect less vegetation and drier conditions.

Annual and interannual water balance. The maximum cumulative subsurface water accessed for evapotranspiration for any consecutive multi-year period (1985–2018) is depicted in Figure 9. A broad belt of substantial interannual subsurface use (200–300 mm yr⁻¹) is evident in the middle elevations of the American River watershed (~800–1300 m), which is largely absent in the Yuba. Upper elevations of both watersheds exhibit little subsurface water accessed for evapotranspiration.

DISCUSSION**Disturbance and management effects on water**

balance. Declines in evapotranspiration make a greater fraction of annual precipitation available for runoff from source-water watersheds to downstream users. Disturbance by wildfire, managed fire, or mechanical thinning lowers evaporative demand, which is proportional to biomass amount, i.e. forest density. The amount that evaporative demand decreases, and the rate of growth in demand as vegetation regrows, also depend on the interaction of climate and geology. While reported fire severity, represented by basal-area reduction, varies from fire to fire (Figure 5), these two densely forested watersheds give 5-year post-fire average values of about 65±32 mm yr⁻¹ reduction (mean ± standard deviation) in ET for each 25% increase in basal-area reduction class (Figure 3). The variability around the mean, shown for the 50–75% line, is expected given the heterogeneity in vegetation density, forest structure, species mix and thus fire response across the basin. Differences in weather between different wildfires, plus landscape attributes also contribute to the observed variability in wildfire response.

The lowest fire-intensity class, 0–25% reduction in basal area, may be considered equivalent to a relatively light management treatment, but one that is realistic for areas where infrastructure or habitat limit actions. A fire in the two medium-intensity classes (25–75%) includes the range considered for restoration

treatments. Our data reflect a five-year mean decrease in ET of about 85 mm yr⁻¹ for 0–25% basal-area removal, versus about 175 mm yr⁻¹ for a 25–75% basal area reduction (Figure 3). Again, variability across forest stands with different elevations, precipitation, subsurface-water storage, and pre-fire density, plus interannual variability in climate, give a standard deviation of about 50% of the mean. Still, these values provide planning scenarios rooted in historical data.

For comparison, it is useful to consider some broader assessments of data from other regions that reported changes in evapotranspiration with reductions in forest density. The broad synthesis of data by Zhang et al. (2001), using the Budyko framework, provides an indication of the potential water impacts of forest management. Using equation 8 in Zhang (2001) with the average annual precipitation for the two basins for the study period (1479 mm for the Yuba and 1228 mm for the American), a 50% reduction in forest cover, replaced by grassland vegetation, gives a 167 mm and 136 mm reduction in annual ET, respectively. Each 25% reduction in forest density provides about a 77 mm reduction in annual ET. These numbers are remarkably similar to the averages apparent in our data (Figure 3), which give an average of 68 mm yr⁻¹ across the study area, and about 83 mm yr⁻¹ for the elevations having the most area burned.

The large variability in rates of post-fire recovery of evapotranspiration toward pre-fire levels is also expected, given the variability of wildfire patterns across the different fires aggregated in this analysis, the interannual variability in climate following the different fires, and the heterogeneity of landscape attributes across the steep gradients in mountains such as the Sierra Nevada. While individual wildfires showed a range of ET recovery rates and amounts (Figure 5), an overall examination of post-fire evapotranspiration recovery amounts suggests little influence of precipitation and temperature (elevation), at least for the first five years post fire (data not shown). Nevertheless, the consistency in rates for the 2 medium-intensity classes, especially in the American, 6.4 mm yr⁻¹, provide planning values based on past climate (Figure 4). Values in the Yuba were higher, 8.8–10.5 mm yr⁻¹, but dominated by one large lower-elevation fire in an area with higher precipitation. The future rate of post-fire recovery will depend on the sequence of wet and dry years, particularly for areas with higher dependence on interannual subsurface water storage (Figure 9).

The net observed changes in *ET* over the two basins, when expressed as changes in *P-ET*, are relatively small compared to the whole-basin discharge. The net reduction in the American basin for the decade ending in 2013, before the 2014 King Fire, averaged about 40 million m³ yr⁻¹ (Figure 7a), compared to an average annual basin discharge over that period of 2849 million m³ yr⁻¹. Even the value of about 100 million m³ yr⁻¹ in 2018 is still under 4%, and not detectable in flow measured at the basin outlet.

The Yuba and American watersheds have higher *P*, *ET* and *P-ET* values compared to areas further south in the Sierra Nevada (Bales et al., 2018), suggesting that there is significant potential for higher gains in *P-ET* and thus runoff from forest management. For example, sustained *ET* reductions at the level shown on Figure 6, averaging over 50 mm yr⁻¹ for 25–75% basal-area reduction for the 1985–2013 period, could have a significant impact if extended over a larger areas. Sustaining that amount over 50% of the American and Yuba basins would reduce evapotranspiration and provide potential runoff by about 121 and 72 million m³ yr⁻¹ in the two basins, respectively, or about 4% of each basin's average discharge over our 1985–2008 study period. Applying the higher average amounts of *ET* reduction observed in both basins in the 25-year period shown on Figure 7b, 131 mm yr⁻¹, would give about reductions in *ET* and potential runoff of about 10% of the period-average discharge, totaling about 0.5 billion m³ yr⁻¹ for the two basins. It is acknowledged, however, that extending treatments over large areas of the Sierra Nevada is constrained by multiple factors (North et al., 2015b).

Subsurface storage and resistance to dry periods. In California's Mediterranean climate, snowpack and subsurface water storage provide the water needed to sustain ecosystems during the summer-fall dry period. For higher elevations, which are also cold during the wet winter season, the dry period is the main period of growth. Vegetation densities are thus controlled in part by climate, i.e. temperature and precipitation, and also by the interaction of climate with weathered bedrock over geologic time. The vulnerability of forests to drought then occurs with a shortage of precipitation, warmer temperatures and limited subsurface storage.

In a multi-year drought, precipitation may be less than the level of evapotranspiration needed to sustain a forest, with multi-year subsurface storage making up the difference. However, there is a limit to how many

years and how much water deficit can be met from storage before root-zone water storage is depleted (Klos et al., 2018). As temperature warms, the evaporative demand of existing vegetation can increase (Goulden and Bales, 2019). Warmer temperatures also shift precipitation from snow to rain, and melt snow earlier in the year, resulting in longer reliance on subsurface water storage for the growing season. Thus subsurface storage is expected to support less summer evaporative demand by vegetation as climate warms, versus in the past.

Broad areas of the upper Yuba appear to have substantial annual subsurface storage (Figure 8) and during the period of analysis drew upon minimal interannual (over-year) subsurface storage (Figure 9). That is, current forest water use is well within precipitation amounts at all elevations, and forests are able to tap substantial subsurface water storage during warm and dry periods each summer. Interannual storage is more important at lower elevations where there is less rain, however these areas also have low *ET* values (Figures 2 and S4).

The main area exhibiting potential vulnerability to multi-year dry periods is the broad middle portion of the American River basin (Figure 9), in the 600–1200 m elevation range (Figure 1). A cumulative interannual deficit of 300 mm in subsurface storage should not affect the seasonal demand to sustain summer evapotranspiration, provided root-accessible water is greater than the sum of the interannual deficit and the seasonal *ET* supported by storage, on the order of 600 mm. As reported for the further-south Kings River basin, the forest at 1160 m elevation had a *P-ET* deficit approaching 1500 mm when tree mortality became widespread (Goulden and Bales, 2019). Indications are that moisture stress may have started when the *P-ET* deficit surpassed 1000 mm. Thus the American basin has some additional resilience, but should see greater drought stress for a more-sustained, warmer or drier drought than in the period fall 2011 to fall 2015.

It is also important to emphasize that for projecting drought stress, cumulative *P-ET* deficit (Figure 9) has been shown to be well correlated with indices of drought stress and tree mortality such as satellite-derived normalized difference moisture index (NDMI) and aerial surveys done by the U.S. Forest Service (Goulden and Bales, 2019). Traditional indices such as Standardized Precipitation Index (SPI), Standardized Precipitation Evapotranspiration Index (SPEI) and Palmer Drought Severity Index (PDSI) were not well correlated with forest stress or mortality in the Sierra

Nevada during the recent 4-year drought. When used together with seasonal demand for subsurface water to support evapotranspiration (Figure 8), cumulative $P-ET$ deficit (Figure 9) can be applied more broadly to anticipate drought stress and focus forest-management priorities.

Water-balance uncertainty. As a check on the water balance we summed total annual runoff ($P-ET$) per basin, which compared well with full natural flow values from the California Department of Water Resources (Figure 10). The $P-ET$ values exhibit a median bias of about 130 mm for the Yuba and 40 mm for the American. These values, about 5% of precipitation or 10% of full natural flow, are within the expected uncertainty of the analysis. Note that annual values of $P-ET$ do not account for ΔS , which is reflected in dry years having slightly higher runoff than would occur in the absence of multi-year storage to support ET. Conversely, in wet years some precipitation will go to replenishing over-year storage deficits, especially when following multi-year dry periods (Bales et al., 2018). However, in these basins, interannual ΔS during the study period was relatively small (Figure 9).

In the current analysis we used the 2-variable model (NDVI and precipitation) for scaling the analysis of drought stress, and continue the NDVI-only model for assessing response to disturbance. The 2 variables in our additive model are weakly correlated in the calibration data ($r^2 = 0.33$). Given the weighting between the additive terms in the 2-variable model, the ET response to NDVI changes is muted compared to the one-variable model.

In prior analyses, the NDVI-only model worked well for water balance in the southern Sierra (Bales et al., 2018), and provided an index for projecting forest drought stress (Goulden and Bales, 2019). Yet in the current water-balance analysis it underestimates evapotranspiration across higher-precipitation basins, giving median bias values of 300 and 170 mm for $P-ET$ versus full-natural flow for the Yuba and American, respectively. The two-variable additive model (NDVI and precipitation) gave respective average ET values for the two watersheds of 668 and 610 mm yr⁻¹, versus 461 and 432 for the NDVI-only model. These latter values are essentially the same as those from a large-scale blended satellite-data and bottom-up modeling approach, which reported evaporation estimates across California (Baldocchi et al., 2019). Their average ET values for the 2 watersheds were 460 and 454 mm yr⁻¹, respectively.

Another difference between the results from Baldocchi et al. (2019) versus our statistical approach is the pattern of ET. Their results show less difference in modeled ET across areas with different NDVI, precipitation and temperature compared to our statistical approach.

The basin water balance on Figure 10 shows that $P-ET$ values during dry years have a relatively small bias compared to flow measured at the basin outlet, reflecting evapotranspiration in drier parts of the basin depending on multi-year subsurface water storage to make up for deficits in precipitation. In wet years, the bias in $P-ET$ relative to full natural flow is larger, part of which should reflect replenishment of subsurface storage that was drawn down in wetter years. Overall, however, there is little evidence for water limitation basin wide. The implication for forest restoration is that reductions in forest density by management actions or wildfire should reduce forest evapotranspiration, as remaining vegetation is not water limited (Saksa et al., 2019). Forest treatments, therefore, will not only increase runoff by reducing ET, but also have the potential to increase subsurface storage of water in dry years. This increase should lead to increases in runoff in current or subsequent years, increase minimum flows, and increase forest water availability.

Limitations of analysis. An interesting result of this work is that net evapotranspiration change due to fire in the American River watershed was approximately 20% less than that reported by Roche et al. (2018). This is the result of i) using the USGS Tier 1 Collection 1 of Landsat data versus the Pre-collection data, ii) using a normalization that is more representative of the entire vegetation range of California than that of Su et al. (2017). While there may be an impact to the annual NDVI average due to variable snow and cloud cover filtering of mid- and high-elevation areas, the improved regression results relative to that used earlier gives us confidence in the current results. Note that the current regression has additional years of data not available for the earlier analysis. Additional work is needed to characterize the difference between an unweighted mean NDVI as used here versus a smoothed and month-centered NDVI average as used in Roche et al. (2018).

This analysis assumed that all unburned forested polygons represented control conditions even though some proportion had been logged or mechanically thinned during the analysis period. The effect of this known issue would be to reduce the estimate of

evapotranspiration reduction due to fire. With respect to these limitations, it can be stated that the results should represent conservative estimates of potential ET reductions due to forest thinning through fire.

An additional limitation is the neglect of net lateral subsurface flow between cells. Subsurface redistribution of water would result in some cells having more and some less water for evapotranspiration than indicated by annual precipitation. While a comprehensive spatial analysis of the question has yet to be reported for Sierra Nevada basins, both measurements and modeling point to the effect being relatively small across most of the landscape. This does not rule out local hotspots where lateral redistribution is important, given its importance in sustaining baseflow in streams and dry-season evapotranspiration. In a southern Sierra headwater catchment, Oroza et al. (2018) found topographic wetness index (TWI) to be an explanatory variable for spatial patterns of soil-water storage only during the dry summer period, after drawdown of soil water following the wet winter and spring periods. Similarly, across a broad area of the southern Sierra, Su et al. (2017) found that TWI was not a good predictor of patterns in moisture stress (NDMI) or greenness (NDVI) from Landsat. Using a rich suite of soil-moisture data from headwater catchments in the American and Merced River basins, Saksa et al. (2017) modeled catchment-scale water balances, with no significant lateral redistribution. This is also consistent with extensive subsurface measurements focusing on the 2012-15 drought in the southern Sierra, which showed limited evidence of lateral redistribution (Bales et al., 2018). Lateral redistribution is an inherent limitation in any hydrologic model that accounts for significant amounts of stored water to meet evaporative demands (see Figure 8). Lundquist and Loheide (2011) estimated lateral transfer of subsurface water from high to low elevations to be about 10% of the water balance for the Upper Merced River watershed in the Central Sierra Nevada Mountains of California. Broader and more-thorough examination of when and where this component of the water balance could be important could build on these several studies, particularly the rich spatial data sets now available in the Sierra Nevada.

Finally, while the findings reported here can be used to predict ET response to wildfire and regrowth in these and nearby watersheds, they represent mean historical behavior across several disturbance events. Averaged over longer times and areas, these

predictions can provide useful guides for assessing water-balance response to disturbance and recovery. These top-down modeling results can serve as evaluation data for more process-based, bottom-up modeling. Predictions based on the results presented here also provide important data for resource-management planning and scenario analysis.

CONCLUSIONS

We found that historical wildfire has made significant post-fire reductions in evapotranspiration for at least 5 years in northern Sierra forested watersheds, and in some cases for more than 20 years. However, as the areas affected by wildfire were only a fraction of the larger watersheds in which the fires occurred, the effect on runoff in the two basins studied was somewhat limited. Based on the response of evapotranspiration to the levels of biomass removed in medium-intensity fires (25-75% basal area loss), widespread management actions involving mechanical thinning and controlled burns can have significant local effects on evapotranspiration, with reductions as much as 150-200 mm yr⁻¹ for the first 5 years. For the 2 basins studies, this represents 25-30% of average annual evapotranspiration in productive forests, and has the potential to increase runoff by measurable amounts if extended over as much of the watershed as can be treated. Rates of regrowth in post-wildfire evapotranspiration confirm the need for follow-up forest treatments at intervals of 5-20 years to sustain lower evapotranspiration, depending on local landscape attributes and interannual climate.

The northern-Sierra watersheds studied have experienced little moisture stress during the 1985-2018 period of our analysis, owing to relatively small reliance on interannual subsurface water storage to meet dry-year evapotranspiration needs of vegetation. The cumulative interannual deficits that we found were up to 300 mm yr⁻¹, which are on the order of 25% of the deficits observed in the southern Sierra before widespread tree mortality occurred. However, longer dry periods will push parts of the American River basin toward the thresholds that resulted in widespread forest mortality in the Southern Sierra Nevada. Use of cumulative precipitation minus evapotranspiration (P-ET) provides a good index for planning and assessment.

DATA AVAILABILITY STATEMENT

All data used in this analysis are included in the supplemental materials or are publicly available.

AUTHOR CONTRIBUTIONS

JRo carried out most of the analysis and wrote parts of the manuscript. QM developed the spatial data products. JRu developed the datasets used to develop the spatial data. RB supervised the work and prepared the final manuscript. All authors edited the manuscript.

FUNDING

This research was supported by a USDA Small Business Innovation Research grant to Blue Forest Conservation, with supplemental support from the National Science Foundation through the Southern Sierra Critical Zone Observatory (EAR-1331939), from the Nature Conservancy, and from the California Strategic Growth Council through the Innovation Center for Ecosystem Climate Solutions.

ACKNOWLEDGEMENTS

The authors wish to acknowledge constructive comments from the reviewers, which guided improvements to the manuscript. This research was supported by a USDA Small Business Innovation Research grant to Blue Forest Conservation, with supplemental support from the National Science Foundation through the Southern Sierra Critical Zone Observatory (EAR-1331939), from the Nature Conservancy, and from the California Strategic Growth Council through the Innovation Center for Ecosystem Climate Solutions. Eddy-covariance data are available at <https://ameriflux.lbl.gov/>. PRISM data are accessible at <http://www.prism.oregonstate.edu/>. Landsat data are available at <https://www.usgs.gov/land-resources/nli/landsat/landsat-collection-1-surface-reflectance>. Unimpaired runoff data are accessible at <https://cdec.water.ca.gov/>. SRTM data were used for elevations, and are available at <https://www2.jpl.nasa.gov/srtm/>

SUPPLEMENTARY MATERIAL

The Supplementary Material for this article can be found online at: <https://www.frontiersin.org/articles/10.3389/ffgc.2020.00069/full#supplementary-material>

REFERENCES

- Google Earth Engine Team. (2015). Google Earth Engine : A planetary-scale geospatial analysis platform. Retrieved from <https://earthengine.google.com>
- Allen, C.D., Macalady, A.K., Chenchouni, H., Bachelet, D., McDowell, N., Vennetier, M., et al. (2010). A global overview of drought and heat-induced tree mortality reveals emerging climate change risks for forests. *For. Ecol. Manag.*, 259(4), 660–684. doi:10.1016/j.foreco.2009.09.001.
- Anderegg, W.R.L., Kane, J. M. & Anderegg, L. D. L. (2013). Consequences of widespread tree mortality triggered by drought and temperature stress. *Nat. Clim. Change*, 3(1), 30–36. doi:10.1038/nclimate1635.
- Anderegg, W.R.L., Hicke, J.A., Fisher, R.A. Allen, C.D. (2015). Tree mortality from drought, insects, and their interactions in a changing climate. *New Phytol.* 208, 674–683, doi:10.1111/nph.13477
- Baldocchi, D., Dralle, D., Jiang, C. & Ryu, Y. (2019). How much water is evaporated across California? A multiyear assessment using a biophysical model forced with satellite remote sensing data. *Water Resour. Res.*, 55, 2722–2741. doi:10.1029/2018WR023884
- Bales, R.C., Goulden, M.L., Hunsaker, C.T., Conklin, M.H., Hartsough, P.C., O'Geen, A.T., Hopmans, J.W. and Safeeq, M. (2018). Mechanisms controlling the impact of multi-year drought on mountain hydrology. *Sci. Rep.*, 8(1), doi:10.1038/s41598-017-19007-0.
- Barnett, T.P. Adam, J.C. & Lettenmaier, D.P. (2005). Potential impacts of a warming climate on water availability in snow-dominated regions. *Nature*, 438(7066), 303–309. doi:10.1038/nature04141.
- Bosch, J.M. & Hewlett, J.D. (1982). A review of catchment experiments to determine the effect of vegetation changes on water yield and evapotranspiration. *J. Hydrol.*, 55(1–4), 3–23. doi:10.1016/0022-1694(82)90117-2.
- California Data Exchange Center (2019). Available online at <http://cdec.water.ca.gov/dynamicapp/selectQuery> (Accessed 6 Oct. 2019).
- Carlson, T.N. and Ripley, D.A. (1997), On the relation between NDVI, fractional vegetation cover, and leaf area index, *Remote Sens. Environ.*, 62, 241–252. doi:10.1016/S0034-4257(97)00104-1.
- Chen, J.M., Chen, X., Ju, W. & Geng, X. (2005). Distributed hydrological model for mapping evapotranspiration using remote sensing inputs. *J. Hydrol.*, 305(1–4), 15–39. doi:10.1016/j.jhydrol.2004.08.029.
- Dingman, S.L. (2002) Physical Hydrology. 2nd Edition, Prentice Hall, Upper Saddle River, 646 p.
- Fellows, A.W., and Goulden, M.L. (2017). Mapping and understanding dry season soil water drawdown by California montane vegetation. *Ecohydrol.*, 10(1), e1772. doi:10.1002/eco.1772.
- Gholz, H.L. (1982), Environmental limits on above-ground net primary production, leaf-area, and biomass in vegetation zones of the pacific northwest, *Ecology*, 63, 469–481. doi:10.2307/1938964.
- Google Earth Engine Team. (2015). *Google Earth Engine: A planetary-scale geospatial analysis platform*. Retrieved from: <https://earthengine.google.com>.
- Goulden, M. L. (1996). Carbon assimilation and water-use efficiency by neighboring Mediterranean-climate oaks that differ in water access. *Tree Physiol.*, 16(4), 417–424.
- Goulden, M.L., Anderson, R.G., Bales, R.C., Kelly, A.E., Meadows, M., and Winston, G.C. (2012). Evapotranspiration along an elevation gradient in California's Sierra Nevada. *J. Geophys. Res. - Biogeosci.*, 117(G3), doi:10.1029/2012JG002027.
- Goulden, M.L. and Bales, R.C. (2014). Mountain runoff vulnerability to increased evapotranspiration with vegetation expansion. *Proc. Natl. Acad. Sci.*

- USA, 111(39), 14071–14075.
doi:10.1073/pnas.1319316111.
- Goulden, M. L. and Bales, R. C. (2019). California forest die-off linked to multi-year deep soil drying in 2012–2015 drought. *Nat. Geosci.* 12, 632–637 (2019). doi:10.1038/s41561-019-0388-5.
- Grier, C.C. and Running S.W. (1977), Leaf area of mature northwestern coniferous forests - relation to site water-balance, *Ecology*, 58, 893–899. doi:10.2307/1936225.
- Groeneveld, D.P., Baugh, W.M., Sanderson, J.S. and Cooper, D. J. (2007), Annual groundwater evapotranspiration mapped from single satellite scenes, *J. Hydrol.*, 344, 146–156. doi:10.1016/j.jhydrol.2007.07.002.
- Homer, C.G., Dewitz, J., Yang, L., Jin, S., Danielson, P., Xian, Coulston, J., Herold, N., Wickham, J. & K. Megown (2015). Completion of the 2011 National Land Cover Database for the conterminous United States – representing a decade of land cover change information, *Photogramm. Eng. Remote Sensing*, Vol. 81, 345–353. doi:10.3390/rs6087424.
- Klos, P.Z., Goulden, M.L., Riebe, C.S., Tague, C.L., O’Geen, A.T., Flinchum, B.A., et al. (2018). Subsurface plant-accessible water in mountain ecosystems with a Mediterranean climate. *WIREs Water*, 5(3), e1277. doi:10.1002/wat2.1277.
- Lundquist, J.D., & Loheide, S.P. (2011). How evaporative water losses vary between wet and dry water years as a function of elevation in the Sierra Nevada, California, and critical factors for modeling. *Water Resour. Res.*, 47(3). doi:10.1029/2010WR010050.
- Lutz, J.A., Van Wagtenonk, J.W., and Franklin, J.F. (2010). Climatic water deficit, tree species ranges, and climate change in Yosemite National Park. *J. Biogeogr.*, 37(5), 936–950. doi:10.1111/j.1365-2699.2009.02268.x.
- McKenzie, D., Gedalof, Z., Peterson, D.L. & Mote, P. (2004). Climatic change, wildfire, and conservation. *Conserv. Biol.*, 18(4), 890–902. doi:10.1111/j.1523-1739.2004.00492.x.
- Miller, J.D., Knapp, E.E., Key, C.H., Skinner, C.N., Isbell, C.J., Creasy, R.M., and Sherlock, J.W. (2009). Calibration and validation of the relative differenced Normalized Burn Ratio (RdNBR) to three measures of fire severity in the Sierra Nevada and Klamath Mountains, California, USA. *Remote Sens. Environ.*, 113(3), 645–656. doi:10.1016/j.rse.2008.11.009.
- Miller, J.D., Collins, B.M., Lutz, J.A., Stephens, S.L., van Wagtenonk, J.W. & Yasuda, D.A. (2012). Differences in wildfires among ecoregions and land management agencies in the Sierra Nevada region, California, USA. *Ecosphere*, 3(9), 1–20. doi:10.1890/ES12-00158.1.
- Miller, J.D. and Quayle, B. (2015). Calibration and validation of immediate post-fire satellite derived data to three severity metrics. *Fire Ecol.* 11(2): 12–30, doi:10.4996/fireecology.1102012.
- Mu, Q., Zhao, M. & Running, S. (2011). Improvements to a MODIS Global Terrestrial Evapotranspiration Algorithm. *Remote Sens. Environ.* 115, 1781–1800. doi:10.1016/j.rse.2011.02.019.
- Naudts, K., Chen, Y., McGrath, M.J., Ryder, J., Valade, A., Otto, J. & Luyssaert, S. (2016). Europe’s forest management did not mitigate climate warming. *Science*, 351(6273), 597–600. doi:10.1126/science.aad7270.
- North, M.P., Stephens, S.L., Collins, B.M., Agee, J.K., Aplet, G., Franklin, J.F. & Fule, P.Z. (2015a). Reform forest fire management. *Science*, 349(6254), 1280–1281. doi:10.1126/science.aab2356.
- North, M. P., Brough, A., Long, J., Collins, B., Bowden, P., Yasuda, D., ... Sugihara, N. (2015b). Constraints on mechanized treatment significantly limit mechanical fuels reduction extent in the Sierra Nevada. *J. Forest.*, 113(1), 40–48. doi:10.5849/jof.14-058.
- Oroza, C.A., Bales, R.C., Stacy, E.M., Zheng, Z. & Glaser, S.D. (2018). Long-term variability of soil moisture in the southern Sierra: Measurement and prediction. *Vadose Zone J.* 17:170178. doi:10.2136/vzj2017.10.0178
- PRISM Climate Group, Oregon State University, <http://prism.oregonstate.edu>, created July 2018.
- Roche, J.W., Goulden, M.L., and Bales, R.C. (2018). Estimating evapotranspiration change due to forest treatment and fire at the basin scale in the Sierra Nevada, California. *Ecohydrol.*, doi:10.1002/eco.1978.
- Rungee, J., Ma, Q., Bales, R., and Goulden, M. (2019). Evapotranspiration response to multiyear dry periods in the semiarid western United States. *Hydrol. Process.*, 32:2, 182–194, doi:10.1002/hyp.13322
- Running, S.W., Nemani, R.R. & Hungerford, R.D. (1987). Extrapolation of synoptic meteorological data in mountainous terrain and its use for simulating forest evapotranspiration and photosynthesis. *Can. J. For. Res.*, 17(6), 472–483. doi:10.1139/x87-081.
- Saksa, P.C., Conklin, M.H., Battles, J.J., Tague, C.L. & Bales, R.C. (2017). Forest thinning impacts on the water balance of Sierra Nevada mixed-conifer headwater basins. *Water Resour. Res.*, 53(7), 5364–5381. doi:10.1002/2016WR019240.
- Saksa, P.C., Bales, R.C., Tague, C.L., Battles, J.J., Tobin, B.W. & Conklin, M.H. (2019). Fuels treatment and wildfire effects on runoff from Sierra Nevada mixed-conifer forests. *Ecohydrol.*, doi:10.1002/eco.2151.
- Su, Y., Bales, R. C., Ma, Q., Nydick, K., Ray, R. L., Li, W., & Guo, Q. (2017). Emerging stress and relative resiliency of Giant sequoia groves experiencing multiyear dry periods in a warming climate. *J. Geophys. Res.-Biogeosci.*, 122, 3063–3075. doi:10.1002/2017JG004005
- Sivapalan, M., Blöschl, G., Zhang, L. & Vertessy, R. (2003). Downward approach to hydrological prediction. *Hydrol. Process.*, 17(11), 2101–2111. doi:10.1002/hyp.1425.
- Tague, C.L., Moritz, M.A. (2019). Plant accessible water storage capacity and tree-scale root interactions determine how forest density reductions alter forest water

use and productivity. *Front. For. Glob. Change*, doi:10.3389/ffgc.2019.00036.

Tague, C.L., Moritz, M.A. & Hanan, E. (2018). The changing water cycle: The eco-hydrologic impacts of forest density reduction in Mediterranean (seasonally dry) regions. *WIREs Water*, doi:10.1002/wat2.1350.

Tague, C.L., McDowell, N.G., Allen, C.D. (2013). An Integrated Model of Environmental Effects on Growth, Carbohydrate Balance, and Mortality of *Pinus ponderosa* Forests in the Southern Rocky Mountains, *PLoS ONE* 8:e80286. doi: 10.1371/journal.pone.0080286.

Westerling, A.L. (2006). Warming and Earlier Spring Increase Western U.S. Forest Wildfire Activity. *Science*, 313(5789), 940–943. doi:10.1126/science.1128834.

Zhang, L., W.R. Dawes, G.R. Walker (2001). Responses of mean annual temperature to vegetation changes at catchment scale. *Water Resour. Res.* 37:701–708. <https://doi.org/10.1029/2000WR900325>

Zierl, B., Bugmann, H. & Tague, C.L. (2007). Water and carbon fluxes of European ecosystems: an evaluation of the ecohydrological model RHESSys. *Hydrol. Process.* 21, 3328–3339. doi: 10.1002/hyp.6540.

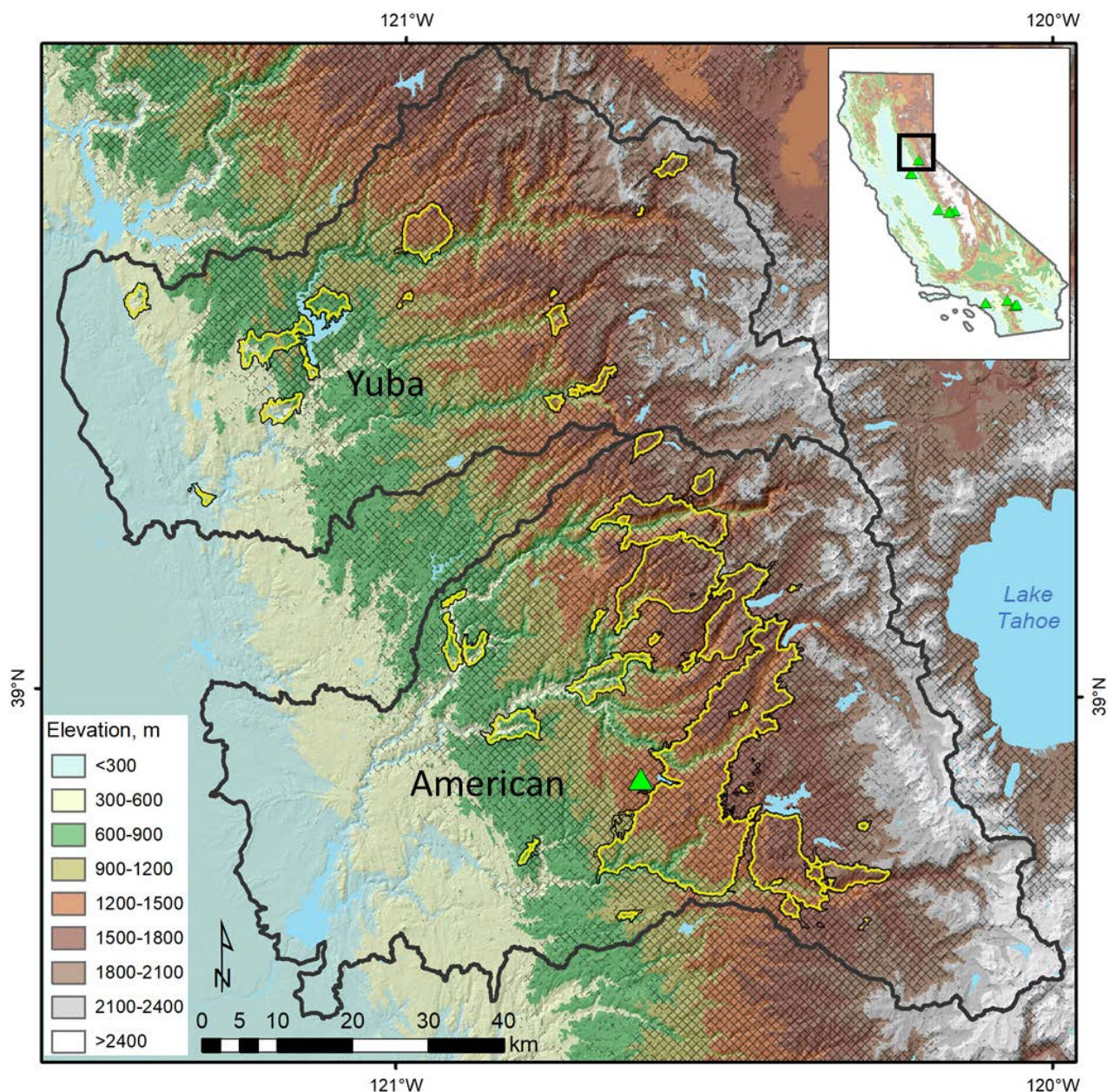


Figure 1. Study area shaded by 300-m elevation bands. Fire perimeters (yellow-black outlines) are all fires to occur in the Yuba and American watersheds greater than 50 ha (1985–2017). Cross-hatching indicates the extent of mixed conifer forest. Inset depicts the study location within the state of California, USA. Green triangles on insert and main map show locations of flux towers used in this study.

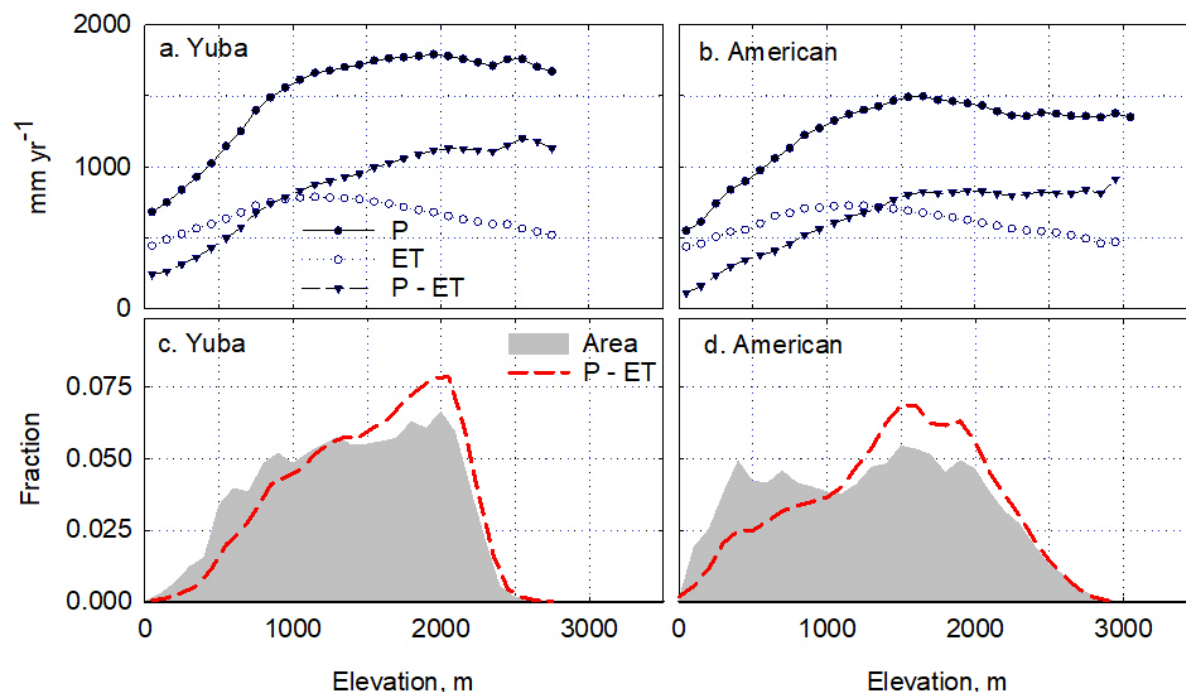


Figure 2. Elevational distribution of mean precipitation (P) and evapotranspiration (ET), and P-ET in the a) Yuba and b) American River watersheds by 100-m elevation bin for the period 1985–2018. Basin-area fraction and volume fraction of P-ET in each 100-m band are shown on panels c) and d). Volume fraction was calculated from depth and area fractions on panels a) and b) See Figure S3 for annual values for an average, wet and dry year.

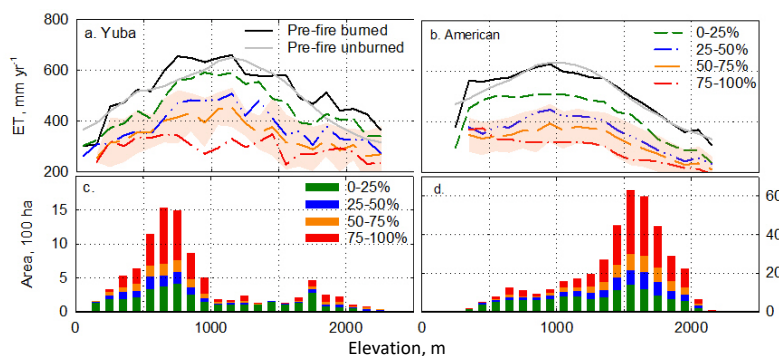


Figure 3. Elevational dependence of 5-year mean evapotranspiration (ET) post forest fire, for fires in the period 1990–2013, categorized by basal-area reduction (fire-severity class): a) Yuba and b) American watersheds. Solid black line is pre-fire ET and solid grey line is control (unburned) area. Shaded area illustrates the standard deviation around the 50–75% basal area reduction line. Other standard deviations are similar. Panels c) Yuba and d) American depict the burned area by basal area reduction quartile class (note the different ordinate scales).

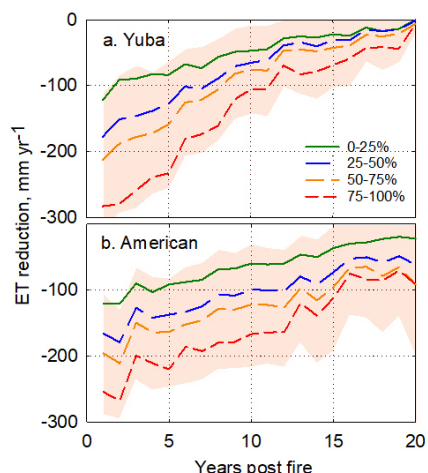


Figure 4. Time series of mean post-fire ET reduction by fire-severity class, or post-fire response of ET, for the a) Yuba and b) American, 1990–2018. Plus and minus one standard deviation is shown for the 50–75% basal-area-reduction class. Other standard deviations are similar.

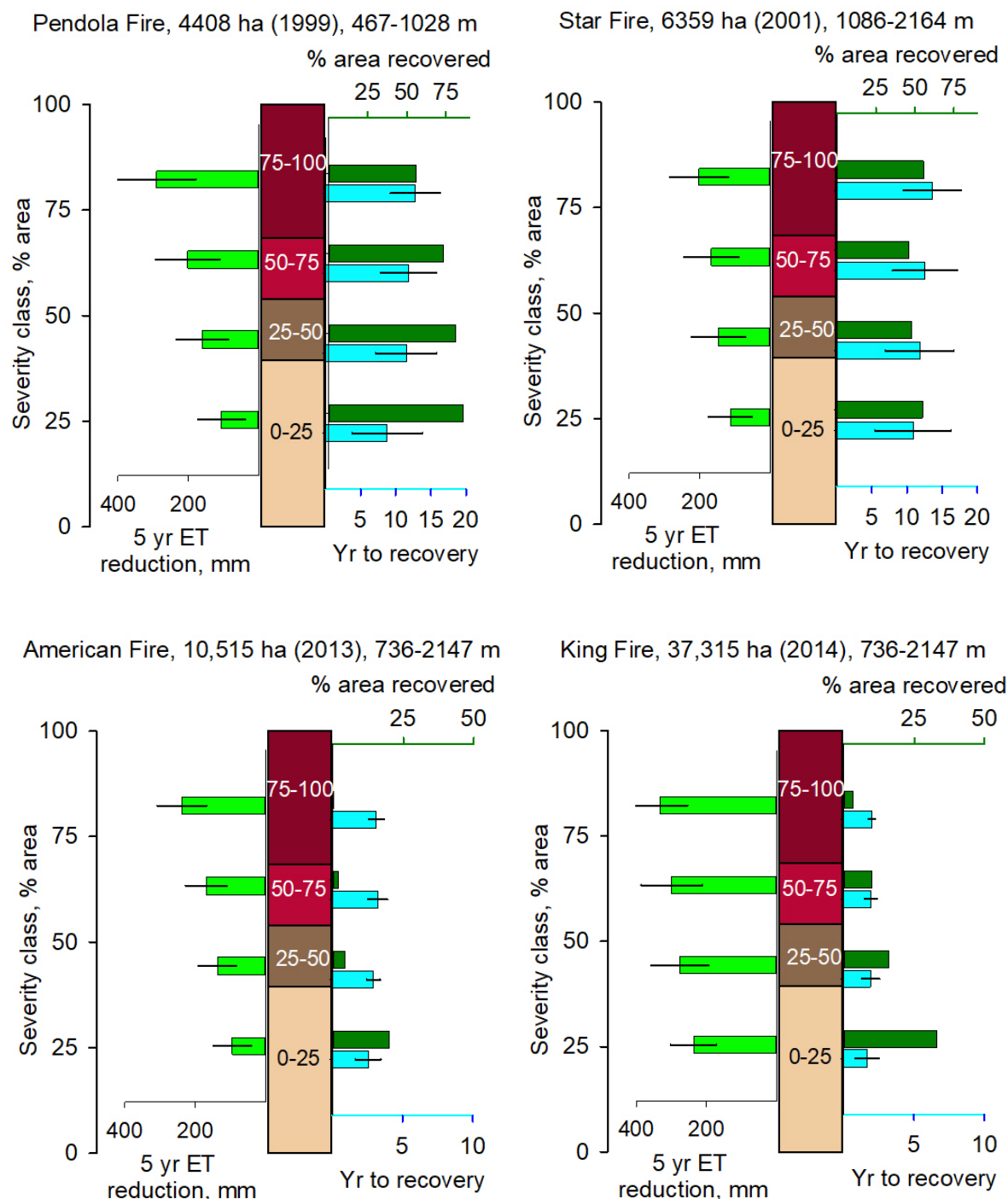


Figure 5. ET reduction and recovery to pre-fire levels for 4 large fires that burned with a range of severity classes. Center, vertical bar shows percent area of fire in each of the 4 severity classes. Bars on the left show ET reduction by fire (mean and standard deviation), averaged over 5 years post fire, by severity class (highest bar is highest severity class). The 4 pairs of bars on the right also correspond to the 4 severity classes, with the upper bar being area recovered and lower bar in each pair being years to recovery of pre-fire ET levels (mean and standard deviation), the number of years to recovery refers only to those grid cells where net ET change is greater than or equal to zero relative to prefire and unburned grid cell ET values (see Equation 5). The remaining grid cells had not recovered as of 2018. The proportion of mixed conifer for each fire is 73% (Pendola), 80% (Star), 83% (King), and 95% (American).

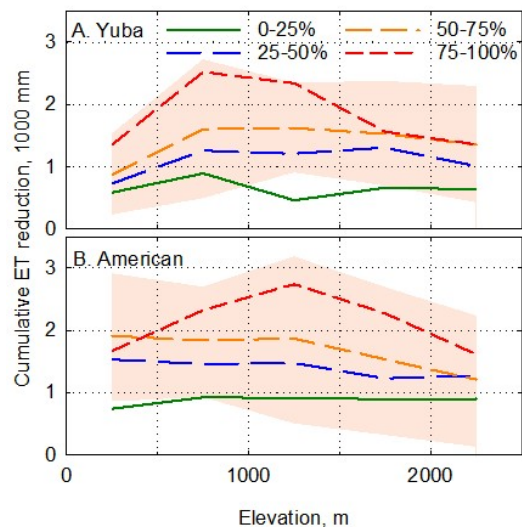


Figure 6. Cumulative ET reduction by fire-severity class and 500-m elevation bins for the a) Yuba and b) American watersheds for fires 1985-2013. Plus and minus one standard deviation is shown for the 50-75% basal area reduction class. Other standard deviations are similar.

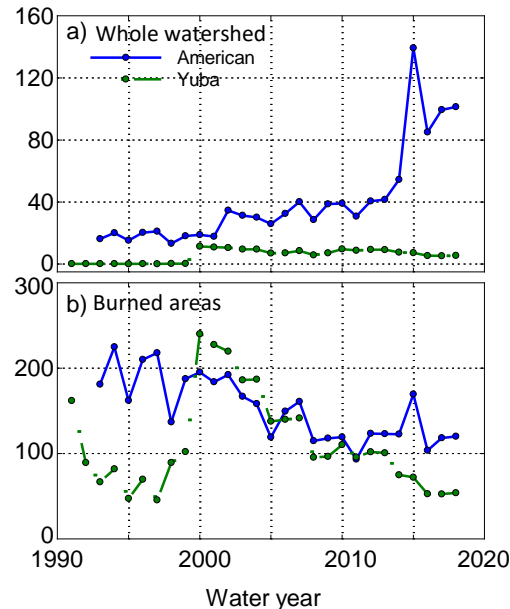


Figure 7. Change in evapotranspiration (ET): a) net whole-basin volumetric change, and b) depth of ET reduction in burned areas (1990-2017) for each watershed.

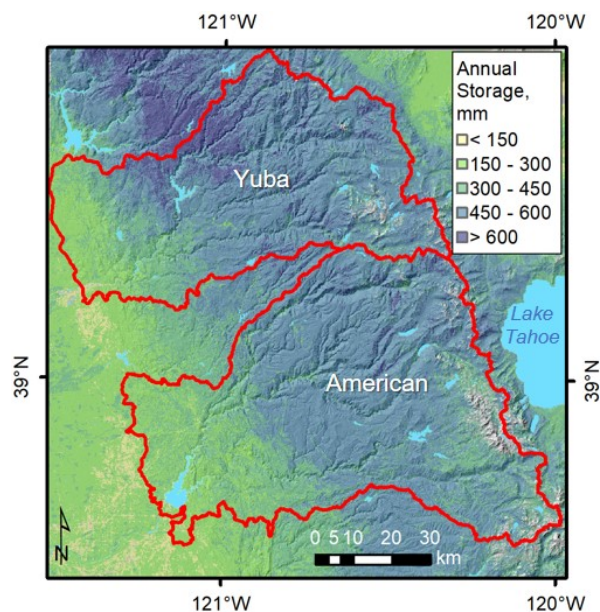


Figure 8. Maximum seasonal amount of subsurface water storage used for evapotranspiration in a single year for the period 1985-2018. Grey area is no data.

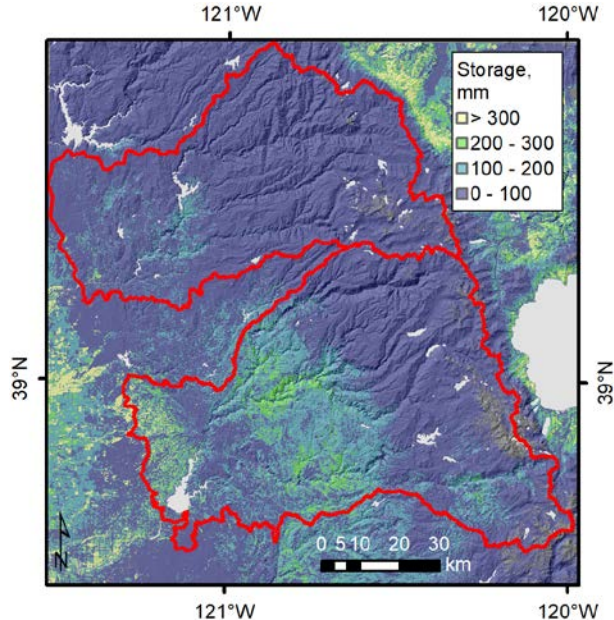


Figure 9. Maximum cumulative (interannual) evapotranspiration supplied by subsurface water storage for the study period (1985-2018), which is the maximum accumulated negative value of annual P-ET. Dark and light grey areas indicate no data and lakes, respectively.

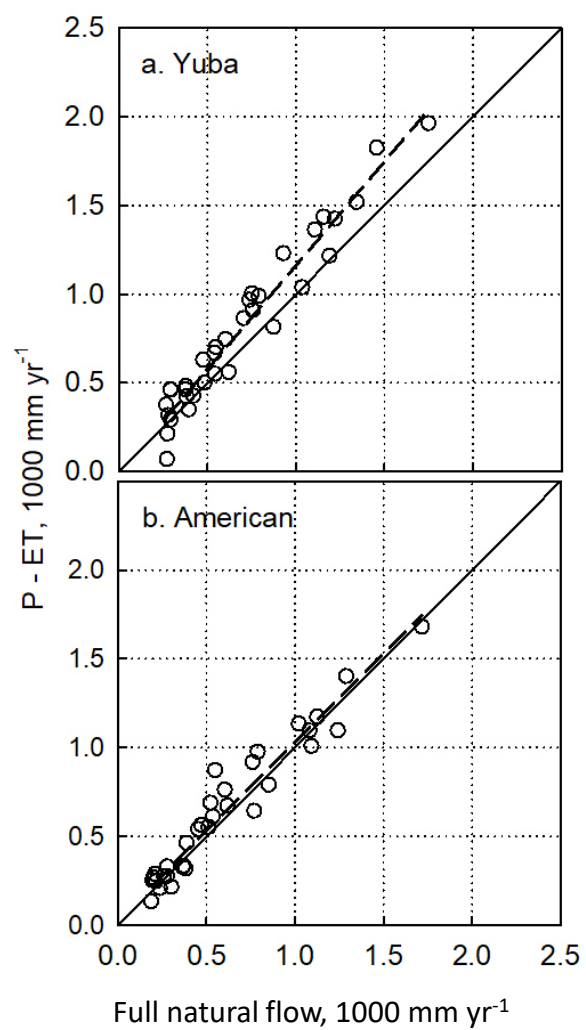


Figure 10. Water balance for the a) Yuba and b) American watersheds (1985-2018). Full natural flow is for the respective USGS stream gage.